THE JOURNAL OF PHYSICAL CHEMISTRY B

Article

pubs.acs.org/JPCB

Solvated Crystals Based on [6,6]-Phenyl-C_{61}-butyric Acid Methyl Ester (PCBM) with the Hexagonal Structure and Their Phase Transformation

Lidong Zheng and Yanchun Han*

State Key Laboratory of Polymer Physics and Chemistry, Changchun Institute of Applied Chemistry, Chinese Academy of Sciences; Graduate University of the Chinese Academy of Sciences, 5625 Renmin Street, Changchun 130022, People's Republic of China

Supporting Information

ABSTRACT: This work focuses on the structural exploration of micro-sized crystals based on a well-known methanofullerene, [6,6]-phenyl-C_{61}-butyric acid methyl ester (PCBM). We have succeeded in producing PCBM crystals with the hexagonal symmetry through the liquid–liquid interfacial precipitation (LLIP) method. We found that smaller but more regular PCBM crystals tend to form in the oversaturated PCBM solutions with solvents of lower solubility for PCBM, such as tetrahydrofuran (THF) and 1,4-dioxane. The structure of the produced crystals also shows a dependence on the solvents, which can be attributed to the incorporation of different solvent molecules into PCBM crystals. Under thermal annealing, for the first time, we have observed a crystalline to crystalline phase transformation of these hexagonal PCBM crystals. Along with the phase transformation, the morphology of the crystals has also been transformed from the hexagon to long needles. In addition, the needlelike crystals arrange themselves with a relative angle of 60° to each other, which implies an intrinsic structural correlation between needlelike and hexagonal crystals.

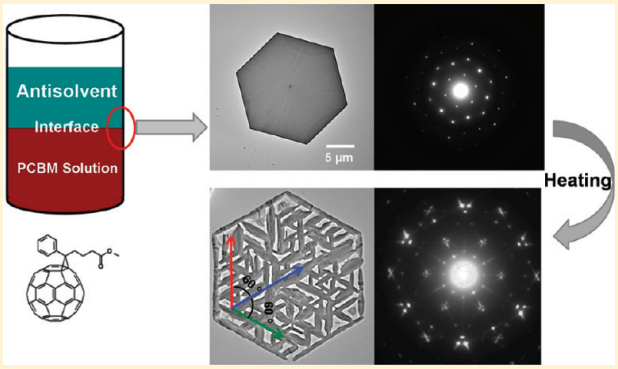

1. INTRODUCTION

Organic semiconducting single crystals exhibit excellent charge-transport properties benefiting from their molecular ordering and the lack of grain boundaries, which attract great attention to the preparation, characterization, and further fabrication of electric devices based on these single crystals.[1] These investigations not only give a direct correlation between the molecular architecture and the molecular packing in their solid states but also shed light on the charge transporting between molecules, which may provide a guideline for the development of organic semiconducting materials from the perspective of molecular architecture and molecular interaction.[2,3] However, preparing single crystals with desired size, shape, and structure is still a great challenge because of the weak interaction between organic molecules and the rigorous condition required for single crystal growth.

The methanofullerene, [6,6]-phenyl-C_{61}-butyric acid methyl ester (PCBM), is considered as a promising semiconducting material with potential applications in both organic photovoltaic solar cells (OPVs)[4] and organic field-effect transistors (OFETs).[5] The advantage of this material lies on that it not only inherits the excellent electric properties of fullerene molecules but also exhibits good solution processability due to the side group attached on the C_{60} molecule.[6] However, the attached side group also makes it harder for PCBM to crystallize than the naked C_{60} molecule.[7] It has been demonstrated that OFET devices based on fullerene in the crystalline state usually have a much higher field-effect mobility than those with fullerene in the amorphous state;[8] therefore, preparing and characterizing PCBM single crystals can not only help to improve their performance in OFET but also can help to give a deeper insight into the electron-transporting processes. For example, it was found that PCBM crystals containing chlorobenzene (CB) molecules with the monoclinic structure formed when it crystallized from CB, while PCBM crystals containing *o*-dichlorobenzene (oDCB) molecules with the triclinic structure formed when it crystallized from oDCB. The structural differences results in a superior OPV performance when using CB as the processing solvent, which benefited from the easier electron hopping in the PCBM crystals within the monoclinic structure.[9] Recently, Dabirian et al.[10] have also reported hexagonal PCBM crystals produced through dip-coating method. They further showed that PCBM crystals could provide a model interface for the fundamental photovoltaic studies after they were coated with electron-donor molecules. However, until now, a facile method for producing PCBM crystals and a further structural investigation focusing on the correlation between different PCBM crystals are still

Received: November 14, 2011
Revised: January 13, 2012
Published: January 19, 2012

   dx.doi.org/10.1021/jp210937h | *J. Phys. Chem. B* 2012, 116, 1598–1604

unavailable, which limits the further exploration of their physical properties.

The liquid−liquid interfacial precipitation (LLIP) method is frequently adopted when preparing organic single crystals because of its easiness to carry out and the well control over the resulted crystals.[11,12] Fullerene crystals with various morphologies and structures have already been prepared directly from its solution by skillfully selecting solvents.[13−21] In this work, a modified LLIP method has been demonstrated to be a facile and effective approach to the preparation of PCBM crystals. By optimizing the preparing condition, micro-sized hexagonal PCBM crystals have been obtained within a few minutes. The morphology and structure of the produced PCBM crystals were found to have a strong dependence on the solvents because of the solubility difference and the incorporation of the solvent molecules in PCBM crystals. Only when tetrahydrofuran (THF) and 1,4-dioxane were used as solvents can hexagonal PCBM crystals with regular shape can be produced in a short time. In addition, a crystalline to crystalline phase transformation around 160 °C from the hexagonal crystals to needlelike crystals was found. The arrangement of those needlelike crystals also have a hexagonal symmetry with three preferred growth directions in the plane parallel to the substrate, which can be attributed to the template effect of the hexagonal single crystals for the needlelike crystals growth.

2. EXPERIMENTAL SECTION

2.1. Materials. PCBM with purity greater than 99% was purchased from Nichem Fine Technology Co. Ltd., Taiwan. The solvents, tetrahydrofudan (THF), 1,4-dioxane, thiophene, chloroform (CF), carbon disulfide (CS_2), toluene, and isopropyl alcohol (IPA) were used as received without further purification.

2.2. Sample Preparation. First, PCBM was dissolved in THF (1 and 2 mg/mL), 1,4-dioxane (1.6 mg/mL), CF (5 mg/mL), thiophene (5 mg/mL), CS_2 (5 mg/mL), and toluene (5 mg/mL) with the assistance of ultrasonic oscillating for 30 min. The resulting solutions were injected into the 4 mL bottles. Then, IPA was slowly added into these bottles along the wall. Those systems were kept still until the precipitation of PCBM crystals. The precipitated crystals were filtered with a 220 μm filter and washed with IPA for several times. At last, they were drop-cast onto copper grid or silica wafer and stored under vacuum for more than 12 h to remove the residual IPA molecules for direct characterization or further thermal annealing treatment. The thermal annealing experiments were conducted on a hot plate in a glovebox.

2.3. Characterization. Optical microscopy images were recorded on an Olympus BX51 system microscopy. TEM images and SAED patterns were obtained with a JEOL JEM-1011 transmission electron microscope operated at an accelerating voltage of 100 kV. The out-of-plane XRD measurement was performed using a Bruker D8 Discover Reflector (Cu Kα, λ = 1.540 56 Å) with generation power of 40 kV tube voltages and 40 mA tube current operated in the locked couple mode. The thermal properties of the PCBM crystals were measured using Perkin-Elmer DSC7 and TGA7 equipment at a heating/cooling rate of 10 °C/min under a nitrogen atmosphere.

3. RESULTS AND DISCUSSION

In the following work, at first, we will demonstrate that the LLIP method can be utilized as an effective approach to the preparation of PCBM crystals. Then, the morphology and structure dependences of these crystals on the processing condition will be investigated. At last, the phase transformation between PCBM crystals with different structures will be discussed.

3.1. Preparing Hexagonal PCBM Crystals through the LLIP Method. The process of preparing PCBM crystals is described in Figure 1a. After PCBM is dispersed in its solvent,

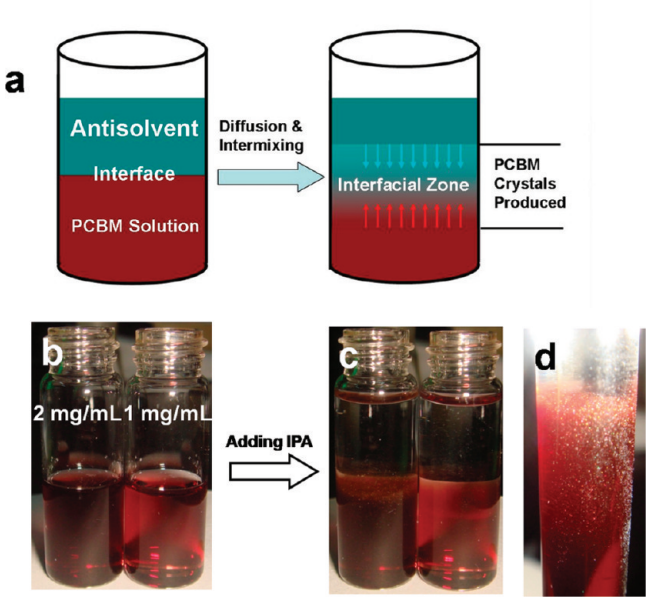

Figure 1. (a) Schematic diagram and (b−d) photographs showing the process of preparing PCBM crystals. (b) PCBM THF solutions with a concentration of 2 mg/mL at left and 1 mg/mL at right. (c) After 2 mL IPA was added into the PCBM THF solution. (d) A magnified photograph showing PCBM crystals produced at the liquid−liquid interface immediately after IPA was added.

the antisolvent, which cannot dissolve PCBM but is miscible with the solvent of PCBM, is injected onto the surface of PCBM solution. Thus, a liquid−liquid interface is formed. The diffusion of the antisolvent into PCBM solution will drive the precipitation of PCBM in the form of crystals. In this work, THF and IPA were selected as the solvent and antisolvent, respectively. After treated by ultrasonic oscillating for 30 min, PCBM has been dispersed in THF (Figure 1b). Then, just after the addition of IPA into this system (v/v = 1/1), the 2 mg/mL PCBM−THF solution becomes turbid immediately (Figure 1c), suggesting the precipitation of PCBM crystals. The magnified photograph in Figure 1d, which focuses on the liquid−liquid interface just after the addition of IPA, shows that there is a concentration gradient of PCBM crystals from the liquid−liquid interface to the interior part of PCBM solution, indicating that the production of PCBM crystals is indeed at the interface. It is quite astonishing to us that the PCBM crystals can precipitate in such a short time just after the IPA addition. However, when saturated PCBM−THF solution (2 mg/mL PCBM solution filtered with a 220 μm filter) or a PCBM−THF solution with a lower concentration (1 mg/mL, right bottle in Figure 1b,c) was used, the precipitating time will be much longer (12 h). These results indicate that the solubility

dx.doi.org/10.1021/jp210937h | J. Phys. Chem. B 2012, 116, 1598−1604

of PCBM in THF must be below 2 mg/mL. Therefore, in the 2 mg/mL PCBM−THF solution, PCBM are not completely dissolved, and after the ultrasonic oscillating treatment, PCBM crystal seeds may exist in the oversaturated PCBM solution (Figure S1). The short precipitating time is due to the existence of those crystals seeds.

The optical and TEM images in Figure 2 show the morphology of the produced PCBM crystals, which maintain

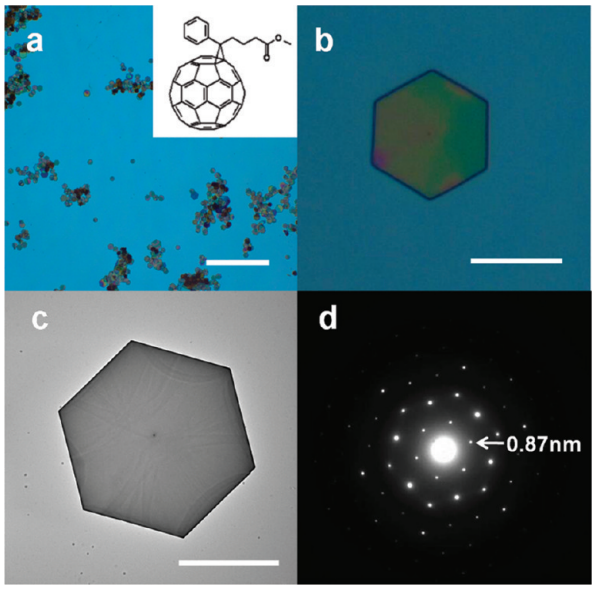

Figure 2. (a, b) Optical microscopic images of PCBM crystals produced through LLIP method. (c) TEM image and the corresponding (d) SAED pattern of the hexagonal PCBM crystals. The inset in (a) is the chemical structure of PCBM. Scale bar = 200 μm in (a) and 10 μm in (b) and (c).

the perfect hexagonal shape with the size of 10−20 μm. The SAED pattern of the hexagonal crystals in Figure 2d also exhibits a hexagonal symmetry. Because all of the hexagonal PCBM crystals flat on the substrate with a unique contact plane, all the peaks on the out-of-plane XRD curve in Figure 3

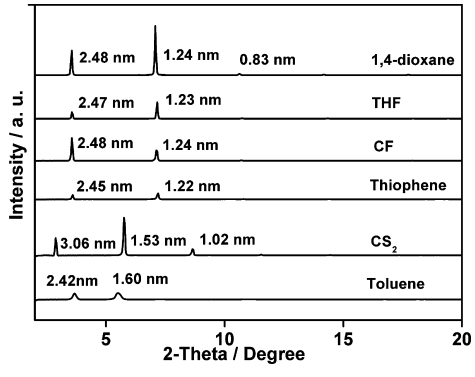

Figure 3. Out-of-plane X-ray diffraction characterization of PCBM crystals on silicon wafer produced through LLIP method with different solvents.

can be attributed to the diffraction from the same crystalline plane with the first-order diffraction corresponding to the *d*-spacing of 2.47 nm. As it is known, the SAED pattern with hexagonal symmetry can only derive from crystals with the cubic or hexagonal structure. However, the possibility of forming cubic PCBM crystals in this work can be excluded by the mismatch of the *d*-spacing of 2.47 nm with the (111) crystalline plane of the assumed cubic unit cells. Therefore, these PCBM crystals can be fitted with the hexagonal lattice with their *c*-axis perpendicular to the hexagonal face of the PCBM crystals, and the *d*-spacing of 2.47 nm can be indexed as the (001) plane. In the past decade, great effort has been contributed to the structural investigation of fullerene, and C_{60} crystals the with face-centered cubic (fcc) structure have been reported.[22−25] In the (111) plane of those crystals, the arrangement of C_{60} molecules also show a hexagonal symmetry with the center-to-center distance between neighboring C_{60} molecules about 1 nm.[25] As PCBM is a molecule composed of a C_{60} cage and an attached tail, it is reasonable to expect the hexagonal packing of PCBM because of the interactions between the C_{60} cages, which will result in a (110) diffraction corresponding to the *d*-spacing of 0.866 nm. Therefore, the *d*-spacing of 0.87 nm in the SAED pattern (Figure 2d) may derive from the (110) diffraction if these PCBM crystals can be fitted with a hexagonal lattice with the lattice constants of a = 1.05 nm and c = 2.47 nm.

The PCBM crystals produced in this work are quite similar to those reported by Dabirian et al.[10] through the dip-coating method. However, the formation of those crystals has a strong dependence on the preparing conditions, including the temperature, the withdrawing speed, and the substrate used, etc. The feature of our method adopted in this work lies on its fast and easiness to carry out, and adopting oversaturated PCBM solution and the ultrasonic oscillating treatment is crucial to achieve this goal.

3.2. Dependence of PCBM Crystals on Solvents. As it is known, the size, shape, and structure of the produced organic crystals through the LLIP method have a strong dependence on the adopted solvents.[12,14,15] Therefore, another five solvents were used to investigate their influences on the produced PCBM crystals (Table 1). The out-of-plane XRD curve in

Table 1. A Summary on the Solvents Used in This Work, Their Solubility for PCBM, and the Concentration (*C*) of PCBM Solution Adopted in the LLIP Method

solvent	THF	1,4-dioxane	CF	thiopehene	CS_2	toluene
solubility (mg/mL)	1.5−2	1−1.6	>10	>10	>20	>10
C (mg/mL)	2	1.6	5	5	5	5

Figure 3 suggests that the crystals produced with 1,4-dioxane, CF, and thiophene also have a unique contact plane with the substrate, and the *d*-spacing corresponding to the first-order diffraction is 2.45−2.48 nm, which is similar to the crystal produced from PCBM THF solution. However, the crystals produced from the PCBM CS_2 solution show a larger *d*-spacing of 3.06 nm, and the crystals produced from the PCBM toluene solution show the *d*-spacings of 2.42 and 1.60 nm, indicating that these crystals maintain different structures with the hexagonal PCBM crystals mentioned above.

Optical microscopy and TEM were applied to further explore their morphological and structural differences. As seen in Figure 4, the crystals produced from 1,4-dioxane, CF, and thiophene also show a regular hexagonal shape with the hexagonal SAED patterns (Figures $4c_1$ and $4c_2$), which agrees

dx.doi.org/10.1021/jp210937h | J. Phys. Chem. B 2012, 116, 1598−1604

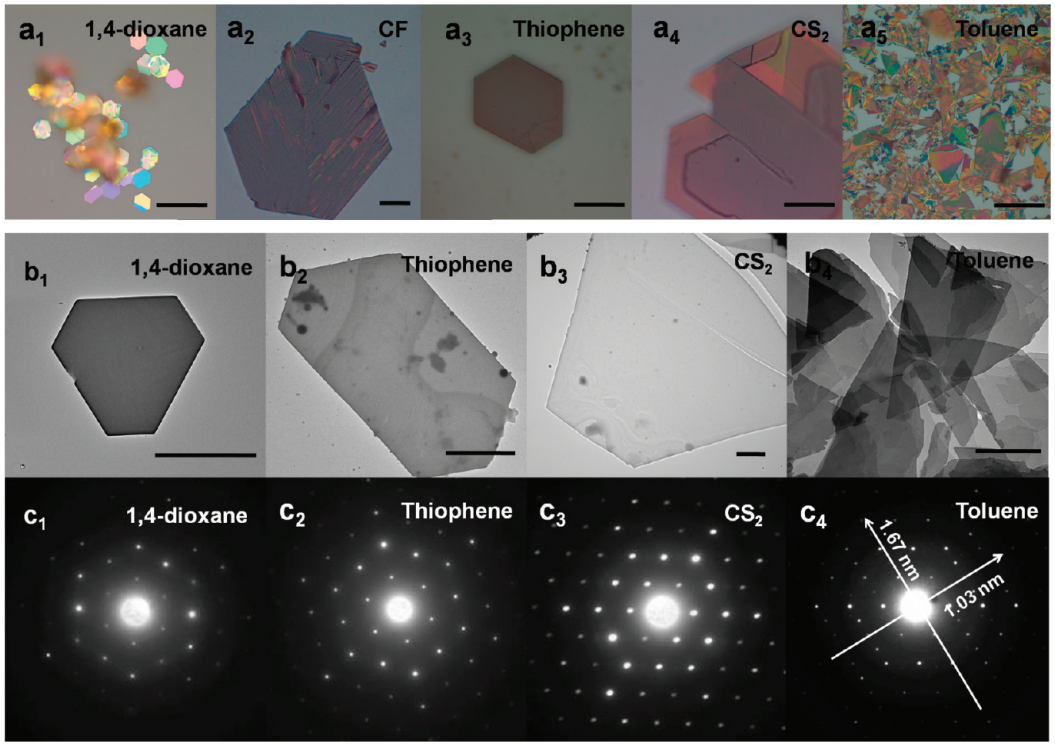

Figure 4. (a_1–a_5) Optical images, (b_1–b_4) TEM images, and the corresponding (c_1–c_4) SAED patterns of PCBM crystals produced through LLIP method with different solvents. Scale bar = 50 μm in (a_1–a_5), 2 μm in (b_1–b_2), and 5 μm in (b_3, b_4).

well with the hexagonal PCBM crystals produced from THF. The difference between these crystals lies on their size and the precipitating time. When preparing PCBM crystals with CF and thiophene, the produced crystals are much larger (up to 100 μm) and the precipitating time is much longer (12 h). This can be attributed to the larger solubility of PCBM in those solvents and the employ of unsaturated PCBM solution (Table 1). The homogeneous nucleation of PCBM in those unsaturated PCBM solutions will be quite difficult and time-consuming, which will result in the production of fewer crystals with larger size in a longer precipitating time. In contrast, using solvents with smaller solubility for PCBM (THF and 1,4-dioxane) and adopting their oversaturated PCBM solution can take the advantage of the existing crystal seeds, which will result in more smaller PCBM crystals in much shorter time. The crystals produced from PCBM CS_2 solution show an irregular shape. Although they have the same SAED pattern (Figure 4c_3) with the crystals produced from PCBM THF solution, they maintain a different crystalline structure because of the larger *d*-spacing in the direction perpendicular to the substrate (Figure 3). As for the crystals produced from PCBM toluene solution, they mainly maintain irregular plates and show an orthotropic SAED pattern with the *d*-spacings of 1.03 and 1.67 nm in the two perpendicular directions (Figure 4c_4).

The above results indicates that the structure of the produced PCBM crystals have a strong dependence on the adopted solvents. A similar phenomenon has been reported when producing C_{60} crystals from different solutions, which is attributed to incorporation of solvent molecules into the crystal lattice.[26−28] The thermogravimetric analysis (TGA) curve in Figure 5a shows that there is a weight loss of 11.72% around 100 °C for the hexagonal PCBM crystals produced through the LLIP method, which cannot be observed for the as-received PCBM powder. These data indicates that the solvent

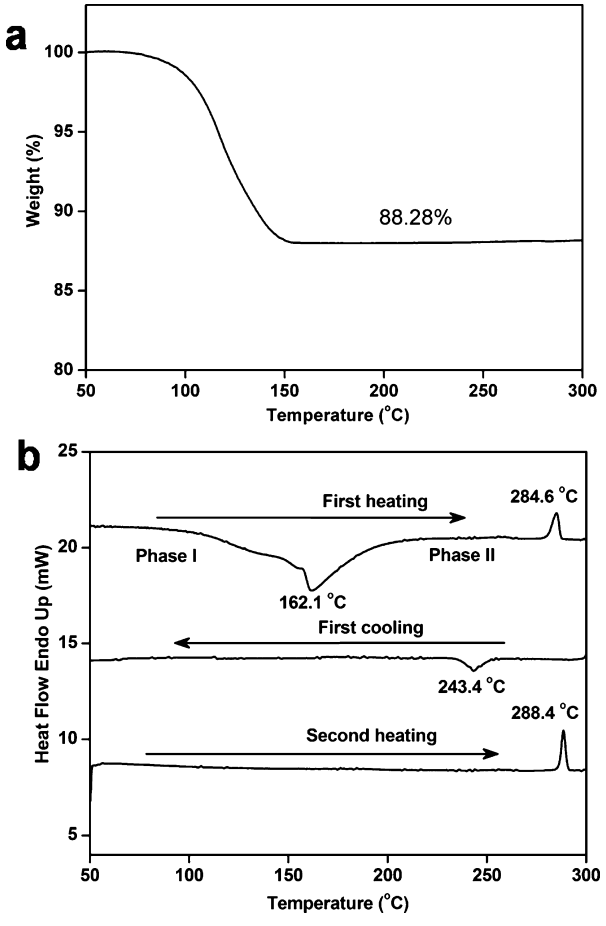

Figure 5. (a) TGA curve and (b) DSC thermograms of the hexagonal PCBM crystals produced through the LLIP method.

dx.doi.org/10.1021/jp210937h | *J. Phys. Chem. B* 2012, 116, 1598–1604

molecules also exist in the crystal lattice of the hexagonal PCBM crystals, and the structure difference between the crystals produced with different solvents may be due to the incorporation of different solvent molecules into PCBM crystals.

3.3. Crystalline to Crystalline Phase Transformation of Hexagonal PCBM Crystals. The DSC technique was applied to investigate the thermodynamics properties of those hexagonal crystals. As shown in Figure 5b, a broad exothermal peak located at 162.1 °C and an endothermal peak around 284.6 °C appear on the first heating curve. Since the sample used for DSC measurement is highly crystalline, the exothermal peak implies that a phase transformation from the hexagonal crystals (phase I) to another crystalline phase (phase II) with better thermal stability may exist. The endothermal peak can be assigned to the melting of that stable crystalline phase. Upon cooling, the exothermal peak located at 243.4 °C corresponds to the crystallization of PCBM from the melting state. But in the second heating process, there is only one endothermal peak at 288.4 °C left. The absence of the exothermal peak around 162.1 °C on the second heating curve suggests that hexagonal PCBM crystals cannot be restored on cooling.

Associated with the crystalline to crystalline phase transformation, the morphology of PCBM crystals also undergoes great changes. The optical and TEM images in Figures 6a and 6b show that after thermal annealing the hexagonal PCBM single crystal (phase I) has been transformed to many needlelike crystals (phase II). Besides, the arrangement of the needlelike crystals still maintains the outline of the original hexagonal crystal, and all the needlelike crystals are highly oriented within the substrate plane with their long axis parallel to one edge of the original hexagonal crystal. Therefore, the hexagonal crystals have passed down their hexagonal symmetry to the orientation of the needlelike crystals during the phase transformation process, which implies that there must be a close correlation between the PCBM crystals with the two different crystalline phases.

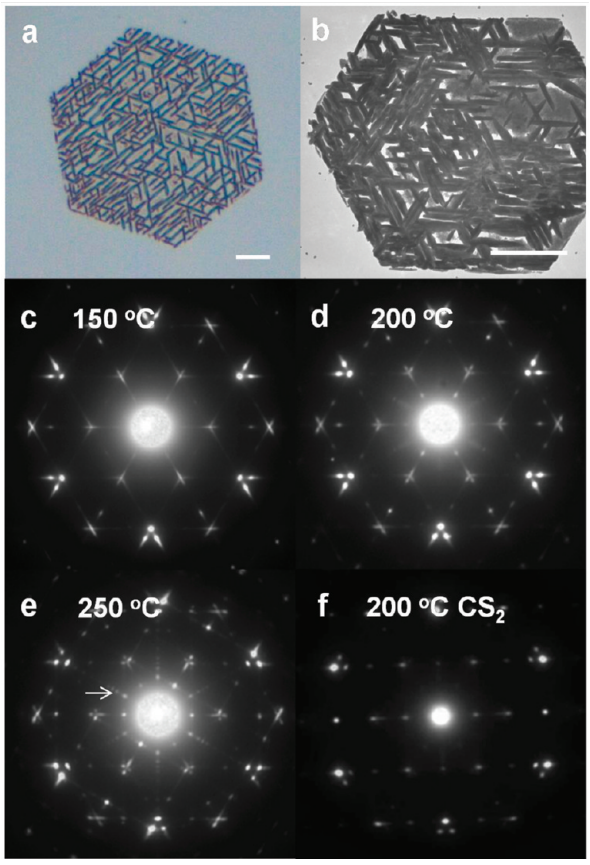

Figure 6. (a) Optical microscopic and (b) TEM images of the hexagonal PCBM crystals after thermal annealed at 200 °C for 10 min. The SAED patterns of the hexagonal PCBM crystals: (c) before and after annealed at (d) 150 °C, (e, g) 200 °C, and (f) 250 °C for 10 min. Scale bar = 5 μm.

To clearly clarify the structural changes of PCBM crystals under thermal annealing, they were further annealed at different temperatures for the SAED characterization. As seen in Figure 6c, after the crystal has been annealed at 150 °C for 10 min, the hexagonal diffraction pattern corresponding to a single crystal has been converted to a complicated pattern with the emergence of several diffraction points around the original point but still maintaining the overall hexagonal symmetry. The blurry diffraction points in Figure 6c become much more identifiable in Figure 6d for the diffraction of PCBM crystals annealed at 200 °C, which suggests the completion of the structure transformation. When further enhancing the annealing temperature up to 250 °C, some additional close-located diffraction points appear, as indicated by the arrow in Figure 6e, while the rest of diffraction points are identical to that in Figure 6d. These data further confirm the structure transformation of PCBM crystals under thermal annealing, which corresponds well with the phase transformation peak located at 162.1 °C on the DSC curve (Figure 5b). Besides, although the diffraction pattern varies with annealing temperature, the morphology of the crystals shows no identifiable differences in the range of 150−250 °C. It should also be noticed that there are also some annealed PCBM crystals which do not show the needlelike morphology as described in Figure 6b but still have the same structure with them (Figure S2). We infer that maybe these crystals are made up of many tiny needlelike crystals which cannot be identified with TEM.

Apparently, every diffraction pattern in Figures 6b−6f originates from the superposition of SAED patterns deriving from the needlelike crystals with different orientations in the plane parallel to the substrate. Figure 7 illustrates the origin of every diffraction points in those patterns. The diffraction pattern in Figure 7b can be divided into three identical orthotropic subpatterns with the unit cell *d*-spacing of 1.01 and 1.51 nm in two perpendicular directions. A relative angle of 60° to each other is formed between the three diffraction subpatterns. This value is the same with the angle between the needlelike crystals in Figure 7a. Therefore, every orthotropic SAED subpattern can be assigned to the diffraction of the needlelike crystals maintaining the same orientation as indicated by arrows in Figure 7a. The SAED pattern (Figure 7d) of the needlelike crystals with the same orientation (Figure 7c) further confirms this conclusion. Besides, in spite of which annealed PCBM crystal was selected for the SAED characterization, we got the same SAED pattern, which indicates that all the needlelike crystals have a unique contact plane with the substrate. Another feature of the needlelike crystals is the big *d*-spacing (5.56 nm) along their long-axis when the annealing temperature is set at 250 °C, as revealed by the close-located diffraction points in Figures 6e and 7d. Although we do not understand the exact origin of those diffractions, we believe that those diffraction points should be attributed to supramolecular

dx.doi.org/10.1021/jp210937h | J. Phys. Chem. B 2012, 116, 1598−1604

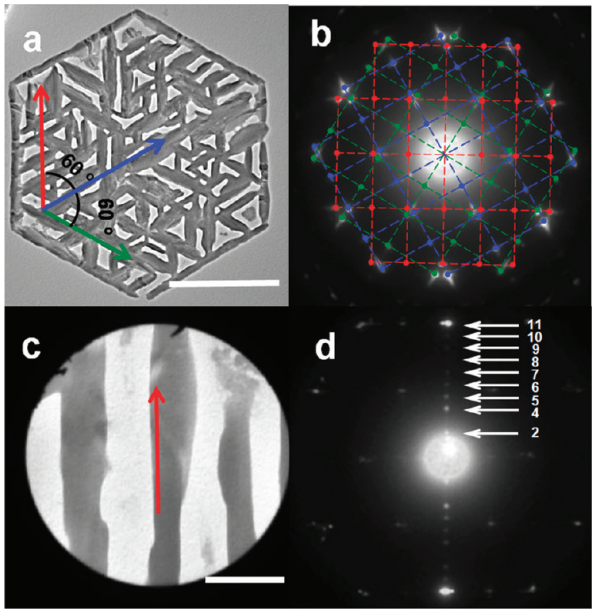

Figure 7. (a) TEM image and the corresponding indexed (b) SAED pattern of the hexagonal PCBM crystals after annealed at 250 °C for 10 min showing that this pattern is made up of three groups of identical subpatterns with a relative angle of 60° to each other. (c) TEM image of selected parts of annealed PCBM crystals with a unique orientation and the corresponding (d) SAED pattern. Scale bar = 5 μm in (a) and 1 μm in (c).

structure formed within PCBM crystals arising from the interaction of the fullerene molecules, just as what we have reported previously.[29]

Another question is why the needlelike crystals arrange themselves with a hexagonal symmetry. We suggest that the interface between the hexagonal and the needlelike crystals in the phase transforming process plays the crucial role. From the relative orientation of the crystals to the substrate, we can infer that both the hexagonal and needlelike crystals have a defined contact plane parallel to the substrate. From the relative orientation of PCBM crystals with respect to each other within the plane parallel to the substrate, we can deduce that there must be a registry between these two kinds of crystals on their contact interface,[30] which can be illustrated in Figure 8. On that interface, the 1 × 3 supercell of the needlelike crystals registers well with the hexagonal surface in the direction parallel to the long axis of the needles. Therefore, the hexagonal PCBM crystals provide a hexagonal template for the growth of the needlelike crystals on them, resulting in the hexagonal symmetry of their orientations.

4. CONCLUSIONS

In this work, a modified LLIP method with the combination of oversaturated PCBM solution and ultrasonic oscillating treatment was applied to the preparation of PCBM crystals, with which hexagonal PCBM crystals can be produced in a few minutes. It was found that the morphology, structure, and precipitating time of the PCBM crystals had a strong dependence on the adopted solvents and the concentration of PCBM solution, which can be attributed to the solubility differences between the adopted solvents for PCBM and the incorporation of the solvent molecules into PCBM crystals. The formation of hexagonal PCBM single crystals suggests that although the C_{60} molecule have been substituted with an asymmetry side-group, fullerene single crystals with hexagonal symmetry can still be produced if the preparing condition is appropriately selected. However, the hexagonal PCBM crystals are not thermal stable and undergo both structural and morphological changes under thermal annealing, with every individual hexagonal single crystal transformed to many orderly arranged needlelike crystals maintaining the original hexagonal outline and the overall hexagonal symmetry. The orderly arrangement of these needlelike crystals can be attributed to the template effect of the hexagonal crystals to the growth of needlelike crystals.

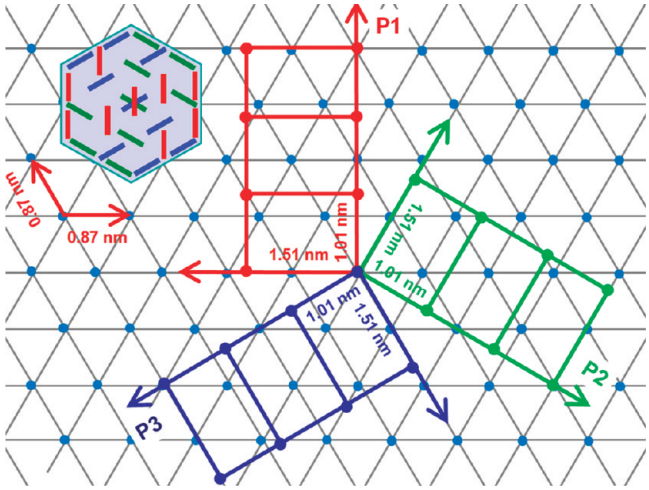

Figure 8. Schematic presentation of contact interface and the relative orientations between the lattices of the hexagonal crystals and the needlelike crystals in that contact interface.

■ ASSOCIATED CONTENT

Ⓢ Supporting Information

TEM image showing the existence of seed crystals in PCBM THF solution; TEM image and SAED pattern showing the annealed PCBM crystals that do not have the needlelike morphology. This material is available free of charge via the Internet at http://pubs.acs.org.

■ AUTHOR INFORMATION

Corresponding Author

*Tel: 86-431-85262175; Fax: 86-431-85262126; e-mail: ychan@ciac.jl.cn.

Notes

The authors declare no competing financial interest.

■ ACKNOWLEDGMENTS

This work was financially supported by the National Natural Science Foundation of China (20621401, 20834005, 51073151) and National Basic Research Program of China (973 Program-2009CB930603).

■ REFERENCES

(1) Briseno, A. L.; Mannsfeld, S. C. B.; Ling, M. M.; Liu, S. H.; Tseng, R. J.; Reese, C.; Roberts, M. E.; Yang, Y.; Wudl, F.; Bao, Z. N. *Nature* **2006**, *444*, 913.

(2) Kennedy, R. D.; Ayzner, A. L.; Wanger, D. D.; Day, C. T.; Halim, M.; Khan, S. I.; Tolbert, S. H.; Schwartz, B. J.; Rubin, Y. *J. Am. Chem. Soc.* **2008**, *130*, 17290.

(3) Tang, Q. X.; Jiang, L.; Tong, Y. H.; Li, H. X.; Liu, Y. L.; Wang, Z. H.; Hu, W. P.; Liu, Y. Q.; Zhu, D. B. *Adv. Mater.* **2008**, *20*, 2947.

(4) Ma, W. L.; Yang, C. Y.; Gong, X.; Lee, K.; Heeger, A. J. *Adv. Funct. Mater.* **2005**, *15*, 1617.
(5) Cho, S.; Seo, J. H.; Lee, K.; Heeger, A. J. *Adv. Funct. Mater.* **2009**, *19*, 1459.
(6) Hummelen, J. C.; Knight, B. W.; Lepeq, F.; Wudl, F.; Yao, J.; Wilkins, C. L. *J. Org. Chem.* **1995**, *60*, 532.
(7) Yang, X. N.; van Duren, J. K. J.; Rispens, M. T.; Hummelen, J. C.; Janssen, R. A. J.; Michels, M. A. J.; Loos, J. *Adv. Mater.* **2004**, *16*, 802.
(8) Chikamatsu, M.; Nagamatsu, S.; Yoshida, Y.; Saito, K.; Yase, K. *Appl. Phys. Lett.* **2005**, *87*, 203504.
(9) Rispens, M. Z.; Meetsma, A.; Rittberger, R.; Brabec, C. J.; Sariciftci, N. S.; Hummelen, J. C. *Chem. Commun.* **2003**, 2116.
(10) Dabirian, R.; Feng, X.; Ortolani, L.; Liscio, A.; Morandi, V.; Mullen, K.; Samori, P.; Palermo, V. *Phys. Chem. Chem. Phys.* **2010**, *12*, 4473.
(11) Sathish, M.; Miyazawa, K. i. *J. Am. Chem. Soc.* **2007**, *129*, 13816.
(12) Sathish, M.; Miyazawa, K. i.; Hill, J. P.; Ariga, K. *J. Am. Chem. Soc.* **2009**, *131*, 6372.
(13) Ji, H. X.; Hu, J. S.; Tang, Q. X.; Song, W. G.; Wang, C. R.; Hu, W. P.; Wan, L. J.; Lee, S. T. *J. Phys. Chem. C* **2007**, *111*, 10498.
(14) Jeong, J.; Kim, W. S.; Park, S. I.; Yoon, T. S.; Chung, B. H. *J. Phys. Chem. C* **2010**, *114*, 12976.
(15) Wakahara, T.; Miyazawa, K.; Nemoto, Y.; Ito, O. *Carbon* **2011**, *49*, 4644.
(16) Jin, Y.; Curry, R. J.; Sloan, J.; Hatton, R. A.; Chong, L. C.; Blanchard, N.; Stolojan, V.; Kroto, H. W.; Silva, S. R. P. *J. Mater. Chem.* **2006**, *16*, 3715.
(17) Wakahara, T.; Nemoto, Y.; Xu, M.; Miyazawa, K.; Fujita, D. *Carbon* **2010**, *48*, 3359.
(18) Ji, H. X.; Hu, J. S.; Wan, L. J.; Tang, Q. X.; Hu, W. P. *J. Mater. Chem* **2008**, *18*, 328.
(19) Miyazawa, K.; Mashino, T.; Suga, T. *J. Mater. Res.* **2003**, *18*, 2730.
(20) Wakahara, T.; Sathish, M.; Miyazawa, K. i.; Hu, C.; Tateyama, Y.; Nemoto, Y.; Sasaki, T.; Ito, O. *J. Am. Chem. Soc.* **2009**, *131*, 9940.
(21) Wang, L.; Liu, B. B.; Liu, D. D.; Yao, M. G.; Yu, S. D.; Hou, Y. Y.; Zou, B.; Cui, T.; Zou, G. T.; Sundqvist, B.; Luo, Z. J.; Li, H.; Li, Y. C.; Liu, J.; Chen, S. J.; Wang, G. R.; Liu, Y. C. *Appl. Phys. Lett.* **2007**, *91*, 103112.
(22) Guo, Y. J.; Karasawa, N.; Goddard, W. A. III *Nature* **1991**, *351*, 464.
(23) Iwasa, Y.; Arima, T.; Fleming, R. M.; Siegrist, T.; Zhou, O.; Haddon, R. C.; Rothberg, R. C.; Rothberg, L. J.; Lyons, K. B.; Carter, H. L.; Hebard, A. F.; Tycko, R.; Dabbagh, G.; Krajewski, J. J.; Thomas, G. A.; Yagi, T. *Science* **1994**, *264*, 1570.
(24) Li, J. Q.; Zhao, Z. X.; Li, Y. L.; Zhu, D. B.; Gan, Z. Z.; Yin, D. L. *Phys. C* **1992**, *196*, 135.
(25) Heiney, P. A.; Fischer, J. E.; McGhie, A. R.; Romanow, W. J.; Denenstein, A. M.; McCauley, J. P.; Smith, A. B. *Phys. Rev. Lett.* **1991**, *66*, 2911.
(26) Yao, M.; Andersson, B. M.; Stenmark, P.; Sundqvist, B.; Liu, B.; Wagberg, T. *Carbon* **2009**, *47*, 1181.
(27) Minato, J.; Miyazawa, K. *Carbon* **2005**, *43*, 2837.
(28) Watanabe, M.; Hotta, K.; Miyazawa, K.; Tachibana, M. *J. Phys.: Conf. Ser.* **2009**, *159*, 012010.
(29) Zheng, L. D.; Liu, J. G.; Ding, Y.; Han, Y. C. *J. Phys. Chem. B* **2011**, *115*, 8071.
(30) Hooks, D. E.; Fritz, T.; Ward, M. D. *Adv. Mater.* **2001**, *13*, 227.